

Analytical infrared intensities for periodic systems with local basis sets

Artur F. Izmaylov and Gustavo E. Scuseria

Department of Chemistry, Rice University, Houston, Texas 77005, USA

(Dated: November 2, 2018)

Abstract

We report a method for the efficient evaluation of analytic infrared (IR) intensities within generalized Kohn–Sham density functional theory using Gaussian orbitals and periodic boundary conditions. A discretized form of the Berry phase is used to evaluate a periodic dipole moment and its derivatives with respect to in-phase nuclear coordinate displacements. Benchmark calculations are presented for one-dimensional chains of water molecules and poly(paraphenylenevinylene).

I. INTRODUCTION

Theoretical prediction of vibrational spectra is a valuable tool for the characterization of compounds and materials which are either not synthesized or difficult to conduct experiments on. It requires at least two types of data: positions of peaks and their intensities. In the vibrational spectroscopy of periodic systems, peak positions are associated with phonon frequencies. Calculation of phonon frequencies from analytical second derivatives have recently become available for Kohn–Sham (KS) density functional theory (DFT) and Hartree–Fock (HF) methods, with plane-waves (PW)^{1,2} and Gaussian type orbitals (GTO).^{3,4} On the other hand, peak intensities have received less attention, even though they are necessary for comparison of theoretical spectra with their experimental counterparts. Part of the problem is that only in the 90’s was their correct theoretical expression derived.^{5,6} Since then, first principle studies with KS-DFT and PWs have become common for infrared (IR) and Raman spectra of solids.^{7,8,9} However, we are aware of only one work on IR intensities with GTOs. Although GTOs have many advantages,^{4,10} especially for orbital dependent functionals, GTO-based techniques are mostly developed in the quantum chemistry community, and therefore, are underrepresented for periodic systems. Thus, in this work, we would like to present a simple scheme for evaluation of IR intensities for periodic systems within KS-DFT and HF with GTOs.

The first order IR intensity of a fundamental transition exciting the j th normal mode is

$$I_j = \frac{N_A \pi}{3c^2} \left(\left| \frac{\partial d_x}{\partial Q_j} \right|^2 + \left| \frac{\partial d_y}{\partial Q_j} \right|^2 + \left| \frac{\partial d_z}{\partial Q_j} \right|^2 \right), \quad (1)$$

where N_A is Avogadro’s number, c is the speed of light, d_{x-z} are the Cartesian components of the dipole moment, and Q_j is the normal mode coordinate.¹¹ Since any normal mode is a linear combination of atomic Cartesian coordinates (\mathbf{R}_i), IR intensities are calculated from $\partial \mathbf{d} / \partial \mathbf{R}_i$. There are two main features arising for these derivatives under periodic boundary conditions (PBC). First, one should consider derivatives with respect to in-phase nuclear coordinate displacements

$$\partial \mathbf{d} / \partial \mathbf{R}_i = \sum_{g=0}^{\infty} \partial \mathbf{d} / \partial \mathbf{R}_{ig}, \quad (2)$$

where g is the index of an unit cell. Although in-phase vibrations do not represent the whole

phonon spectrum of the periodic system, only these vibrations are IR active.¹² Second, under PBC, the dipole moment per unit cell cannot be straightforwardly expressed as a matrix element of the position operator.^{5,6,13,14} According to the modern theory of polarization,^{5,6} the dipole moment per unit cell is a geometric quantum phase or a Berry phase.¹⁵ A non-trivial quantum phase usually appears in cases when the system under study is coupled to the rest of the universe through some external parameter ζ .¹⁶ The Berry phase γ can then be written as

$$\gamma = \text{Im} \oint_{\mathcal{C}} d\zeta \left\langle \psi(\zeta) \left| \frac{\partial \psi(\zeta)}{\partial \zeta} \right. \right\rangle, \quad (3)$$

where $\psi(\zeta)$ is the wavefunction and \mathcal{C} is a closed contour. In the case of periodic dipole moment, the parameter ζ is represented by a reciprocal vector \mathbf{k} running over the Brillouin zone. Therefore, within single-determinant methods, Eq. 3 necessitates evaluating $\partial/\partial\mathbf{k}$ derivatives of the Slater determinant. Since the latter is obtained in the self-consistent field (SCF) procedure which usually adds to the solution arbitrary complex phase prefactors depending on the \mathbf{k} value, it is not trivial to differentiate the SCF solution with respect to \mathbf{k} . Two main approaches to this problem have been proposed. The first method involves a discrete representation of $\partial/\partial\mathbf{k}$ derivatives through matrix elements at neighboring \mathbf{k} points. This representation is invariant with respect to phase arbitrariness which could arise from the SCF procedure.^{5,6} The second approach introduces phase factors which cancel the SCF arbitrary phases and allow one to evaluate $\partial/\partial\mathbf{k}$ by employing regular finite differences techniques.^{17,18,19} Here, we start from the periodic dipole expression arising in the first approach. We consider the first approach as a simpler and computationally more robust alternative, since it does not require introduction of complex phase functions and band resolution techniques. Therefore, it can be seen as a black-box technique that has only the number of \mathbf{k} points in the Brillouin zone sampling as an input. In addition, this method has been tested with plane waves before,^{20,21} and its robustness was demonstrated not only for the linear response regime but for finite electric fields as well. Yet another approach to the periodic dipole derivatives is possible in the case of PWs, where these quantities require only dipole matrix elements between occupied and virtual Bloch functions $\langle \phi_{nk} | \mathbf{r} | \phi_{ak} \rangle$. These “transition” dipole elements can be transformed into the following

well-defined expression^{22,23}

$$\langle \phi_{nk} | \mathbf{r} | \phi_{ak} \rangle = \frac{\langle \phi_{nk} | [H_{\text{SCF}}, \mathbf{r}] | \phi_{ak} \rangle}{\epsilon_a(\mathbf{k}) - \epsilon_n(\mathbf{k})}, \quad (4)$$

where H_{SCF} is the crystal SCF Hamiltonian, $\epsilon_a(\mathbf{k})$ and $\epsilon_n(\mathbf{k})$ are orbital energies of empty and occupied bands. However, in the case of GTOs this approach could be less beneficial since Pulay's type of terms arise. To the best of our knowledge, the only implementation of IR intensities with GTOs was reported by Jacquemin and coworkers²⁴ using the second approach. Thus, the focus of the current work is in adapting the discretized Berry phase approach for evaluation of IR intensities with GTOs.

This work can be also seen as complementary to our previous work on zone centered phonon frequencies.⁴ One should keep in mind that IR intensities are always obtained with vibrational frequencies, and therefore, any algorithm for IR intensities can be seen as an efficient one if its execution time is negligible with respect to that for vibrational frequencies.

II. THEORY

A. Berry phase approach to periodic dipole moment

We first consider the formulation of periodic dipole moment through the Berry phase approach in localized basis sets proposed by Kudin and coworkers.²⁵ We restrict our consideration to closed-shell one-dimensional periodic systems aligned along the z axes. This makes our description simpler without losing essential details. Throughout this work we will be using Bloch orbitals

$$\phi_{nk}(\mathbf{r}) = \frac{1}{\sqrt{N_c}} \sum_{g=0}^{N_c} \sum_{\mu=1}^M \mu_g(\mathbf{r}) C_{\mu n}(k) e^{igka} \quad (5)$$

expanded over Gaussian atomic orbitals (AO) $\mu_g(\mathbf{r})$. Here, small Greek letters are for AO indices with subscripts denoting the unit cell number. In Eq. (5), N_c is the total number of unit cells in the system, $C_{\mu n}(k)$ are crystal orbital (CO) coefficients from the SCF problem under PBC,¹⁰ a is the length of the translational vector, and M is the total number of basis functions per unit cell. The cell-periodic part of a Bloch orbital corresponding to the n th band

$$u_{nk}(\mathbf{r}) = e^{-ikz} \phi_{nk}(\mathbf{r}) \quad (6)$$

can be expanded as

$$u_{nk}(\mathbf{r}) = \frac{1}{\sqrt{N_c}} \sum_{g=0}^{N_c} \sum_{\mu=1}^M \mu_g(\mathbf{r}) C_{\mu n}(k) e^{ik(ag-z)}. \quad (7)$$

According to the Berry phase approach,^{5,6} the z component of the dipole moment per unit cell is

$$d = -\text{Im} \sum_n^{\text{occ.}} \int_{\text{BZ}} dk \int d\mathbf{r} u_{nk}^*(\mathbf{r}) \frac{\partial u_{nk}(\mathbf{r})}{\partial k}. \quad (8)$$

Here, we avoid introducing an additional z subscript, since unless otherwise stated we always will consider the longitudinal part of the dipole moment. Substituting $u_{nk}(\mathbf{r})$ in the dipole expression by Eq. (7) we obtain the following representation for the periodic dipole moment

$$d = d_1 + d_2, \quad (9)$$

$$d_1 = \sum_n^{\text{occ.}} \sum_{\mu,\nu}^M \int_{\text{BZ}} dk C_{\mu n}^*(k) C_{\nu n}(k) \times \sum_g e^{ikga} (Z_{\mu\nu}^{0g} - gaS_{\mu\nu}^{0g}), \quad (10)$$

$$d_2 = -\text{Im} \sum_n^{\text{occ.}} \sum_{\mu,\nu}^M \int_{\text{BZ}} dk C_{\mu n}^*(k) \frac{\partial C_{\nu n}(k)}{\partial k} \times \sum_g e^{ikga} S_{\mu\nu}^{0g}, \quad (11)$$

where

$$Z_{\mu\nu}^{0g} = \int d\mathbf{r} \mu_0(\mathbf{r}) z \nu_g(\mathbf{r}), \quad (12)$$

and

$$S_{\mu\nu}^{0g} = \int d\mathbf{r} \mu_0(\mathbf{r}) \nu_g(\mathbf{r}), \quad (13)$$

are dipole and overlap matrices in the AO basis. Calculation of the d_1 term is more efficient to perform in the AO basis

$$d_1 = \sum_{\mu,\nu,g} P_{\mu\nu}^{0g} (Z_{\mu\nu}^{0g} - gaS_{\mu\nu}^{0g}), \quad (14)$$

where $P_{\mu\nu}^{0g}$ is the electron density matrix. The matrix $(Z_{\mu\nu}^{0g} - gaS_{\mu\nu}^{0g})$ can be further split into Hermitian

$$\tilde{Z}_{\mu\nu}^{0g} = Z_{\mu\nu}^{0g} - \frac{ga}{2} S_{\mu\nu}^{0g} \quad (15)$$

and anti-Hermitian

$$\bar{Z}_{\mu\nu}^{0g} = -\frac{ga}{2} S_{\mu\nu}^{0g} \quad (16)$$

parts. Both matrices $\tilde{Z}_{\mu\nu}^{0g}$ and $\bar{Z}_{\mu\nu}^{0g}$ are real, and we refer to Hermiticity of their reciprocal space counterparts $\tilde{Z}_{\mu\nu}(k)$ and $\bar{Z}_{\mu\nu}(k)$. Since we contract both parts with the Hermitian matrix $P_{\mu\nu}^{0g}$, the anti-Hermitian part can be safely omitted. This leads us to the following working expression

$$d_1 = \sum_{\mu\nu, g} P_{\mu\nu}^{0g} \tilde{Z}_{\mu\nu}^{0g}. \quad (17)$$

The d_2 term requires special care because CO coefficients usually contain arbitrary k -dependent phase factors from a diagonalization procedure. Therefore, one cannot apply regular numerical differentiation schemes directly to CO coefficients. To cope with this difficulty we use a discretization approach²⁵ which starts from rewriting Eq. (11) in the form

$$d_2 = -\text{Im} \int_{\text{BZ}} dk \text{tr} \left[C^\dagger(k) S(k) \frac{\partial C(k)}{\partial k} \right], \quad (18)$$

where only the occupied orbital part of $C(k)$ is engaged. For further discussion we introduce the following O -by- O matrix

$$\Sigma(k, k') = C^\dagger(k) S(k) C(k'), \quad (19)$$

where O is the number of occupied bands. Treating k' as a variable and k as a parameter we can write

$$C^\dagger(k) S(k) \frac{\partial C(k)}{\partial k} = \frac{\partial}{\partial k'} \Sigma(k, k') \Big|_{k=k'}. \quad (20)$$

Keeping in mind the orthogonality relation $\Sigma(k, k) = 1$ we rewrite Eq. 20 as

$$\frac{\partial}{\partial k'} \Sigma(k, k') \Big|_{k=k'} = \frac{\partial}{\partial k'} \ln \Sigma(k, k') \Big|_{k=k'}. \quad (21)$$

The trace operation commutes with the differentiation

$$\text{tr} \left[\frac{\partial}{\partial k'} \ln \Sigma(k, k') \Big|_{k=k'} \right] = \frac{\partial}{\partial k'} \text{tr} [\ln \Sigma(k, k')] \Big|_{k=k'}. \quad (22)$$

Applying the well-known matrix relation $\text{tr} \ln(A) = \ln \det(A)$ to the $\Sigma(k, k')$ matrix we obtain

$$\frac{\partial}{\partial k'} \text{tr} [\ln \Sigma(k, k')] \Big|_{k=k'} = \frac{\partial}{\partial k'} \ln [\det \Sigma(k, k')] \Big|_{k=k'}. \quad (23)$$

Since $\ln \det \Sigma(k, k) = 0$, using simple rectangular discretization for the k' derivatives and the Brillouin zone integration we arrive to the following discretized form²⁵ for d_2 :

$$d_2 = -\text{Im} \sum_{j=1}^{N_k} \ln \det \Sigma(k_j, k_{j+1}) \quad (24)$$

$$= -\text{Im} \sum_{j=1}^{N_k} \ln \det C^\dagger(k_j) S(k_j) C(k_{j+1}). \quad (25)$$

By introducing arbitrary phase factors $e^{i\theta(k_j)}$ in front of CO coefficients, one can easily see that they cancel each other after the summation over the Brillouin zone. Please note that one cannot evaluate Eq. (18) by using a perturbation (linear response) expression to build $C(k + \Delta k)$ from $C(k)$. As was pointed out in Ref. 6, a perturbation theory implicitly uses the so called ‘‘parallel-transport’’ gauge which necessitates phase equality between $C(k)$ and $C(k + \Delta k)$, and as a consequence produces zero Berry phase.

Similar to the molecular case, the transverse components of the periodic dipole moment can be written as

$$d_q = \sum_{\mu\nu, g} P_{\mu\nu}^{0g} Q_{\mu\nu}^{0g}, \quad (26)$$

where $q = x$ or y and

$$Q_{\mu\nu}^{0g} = \int d\mathbf{r} \mu_0(\mathbf{r}) q \nu_g(\mathbf{r}). \quad (27)$$

Therefore, their differentiation is very similar to that of the d_1 part of the longitudinal dipole moment, and it will not be considered further.

B. Dipole derivatives

Differentiation of Eq. (17) with respect to nuclear coordinate displacements gives

$$\frac{\partial d_1}{\partial \mathbf{R}_i} = \sum_{\mu\nu, g} \frac{\partial P_{\mu\nu}^{0g}}{\partial \mathbf{R}_i} \tilde{Z}_{\mu\nu}^{0g} + P_{\mu\nu}^{0g} \frac{\partial \tilde{Z}_{\mu\nu}^{0g}}{\partial \mathbf{R}_i}. \quad (28)$$

Both terms in Eq. (28) are calculated with standard techniques: the coupled perturbed SCF (CPSCF) procedure for the density derivatives,^{4,26} and a regular integral derivatives evaluation technique.²⁷ The CPSCF procedure evaluates the same density derivatives as in

the case of vibrational frequency calculations; therefore computational overhead of the d_1 part is negligible, since it only involves calculation of one-electron terms.

In order to obtain the d_2 derivatives we adapt the algebraic approach discussed in Ref. 20. The main step can be summarized as application of the following algebraic identity

$$\frac{\partial}{\partial \mathbf{R}} \{\ln \det[\Sigma(\mathbf{R})]\} = \text{tr} \left[\Sigma^{-1}(\mathbf{R}) \frac{\partial}{\partial \mathbf{R}} \Sigma(\mathbf{R}) \right], \quad (29)$$

which is an analog of Eqs. 22 and 23. This was proven from a different point of view in Ref. 20. The differentiation of $\Sigma(k_j, k_{j+1})$ gives rise to two types of terms in the d_2 derivatives

$$\frac{\partial d_2}{\partial \mathbf{R}_i} = d_2^{(1)} \left(\frac{\partial \mathbf{S}}{\partial \mathbf{R}_i} \right) + d_2^{(2)} \left(\frac{\partial \mathbf{C}}{\partial \mathbf{R}_i} \right), \quad (30)$$

which correspond to Pulay's type of forces from overlap integral derivatives

$$d_2^{(1)} = -\text{Im} \sum_{j=1}^{N_k} \sum_{m,n}^{\text{occ.}} C_{\mu n}^*(k_j) \frac{\partial S_{\mu\nu}(k_j)}{\partial \mathbf{R}_i} C_{\nu m}(k_{j+1}) \quad (31)$$

$$\times \Sigma_{mn}^{-1}(k_j, k_{j+1})$$

$$= -\text{Im} \sum_{j=1}^{N_k} \sum_{m,n}^{\text{occ.}} \frac{\partial S_{nm}(k_j, k_{j+1})}{\partial \mathbf{R}_i} \quad (32)$$

$$\times \Sigma_{mn}^{-1}(k_j, k_{j+1}),$$

and response of CO coefficients

$$d_2^{(2)} = -\text{Im} \sum_{j=1}^{N_k} \sum_{m,n}^{\text{occ.}} \Sigma_{mn}^{-1}(k_j, k_{j+1}) \quad (33)$$

$$\times \left[\frac{\partial C_{\mu n}^*(k_j)}{\partial \mathbf{R}_i} S_{\mu\nu}(k_j) C_{\nu m}(k_{j+1}) \right.$$

$$\left. + C_{\mu n}^*(k_j) S_{\mu\nu}(k_j) \frac{\partial C_{\nu m}(k_{j+1})}{\partial \mathbf{R}_i} \right].$$

To complete the construction of the dipole moment derivatives we will express CO derivatives via the response matrix U obtained in the CPSCF procedure³

$$\frac{\partial C_{\mu n}^*(k_j)}{\partial \mathbf{R}_i} = \sum_a^{\text{vir.}} U_{na}^*(k_j) C_{\mu a}^*(k_j). \quad (34)$$

Thus we arrive to

$$d_2^{(2)} = -\text{Im} \sum_{j=1}^{N_k} \sum_{m,n}^{\text{occ.}} \sum_a^{\text{vir.}} \Sigma_{mn}^{-1}(k_j, k_{j+1}) \quad (35)$$

$$\times \left[U_{na}^*(k_j) \Sigma_{am}(k_j, k_{j+1}) \right.$$

$$\left. + \Sigma_{na}(k_j, k_{j+1}) U_{am}(k_{j+1}) \right].$$

TABLE I: Optimized geometry (\AA and degrees) of a one-dimensional water chain used to benchmark the accuracy of our analytic method with different basis sets. See Fig. 1 for the definition of the geometrical parameters.

	HF		PBE	
	6-31G	6-311++G**	6-31G	6-311++G**
R_{OH}	0.9625	0.9477	1.0213	0.9843
r_{OH}	0.9492	0.9410	0.9818	0.9692
r_{HO}	1.9084	2.1349	1.6367	1.9158
a	2.7459	2.9547	2.5709	2.8048
α	108.58	104.31	105.77	102.76

Since we do not evaluate \mathbf{R}_i dependent phases, the application of the linear response Eq. (34) is acceptable.

The computational complexity of the presented scheme is negligible with respect to that of vibrational frequency calculations. For the d_2 part we have several matrix multiplications of M -by- M matrices and one O -by- O matrix inversion for each \mathbf{k} point.

Two- and three-dimensional generalizations of the presented method can be done in the same way as for plane-wave implementations; therefore, we refer the interested reader to Ref. 20 for details.

III. BENCHMARK CALCULATIONS

A. Algorithmic tests

To validate and assess the present formalism, which has been implemented in the development version of the GAUSSIAN program,²⁸ we have tested it on a model one-dimensional chain of water molecules (see Fig. 1 and Table I) with the geometry optimized within the HF and PBE methods.²⁹ In order to describe hydrogen-bond interactions properly, we employ the 6-311++G** basis set in most of our tests.³⁰

In Table II we compare dipole derivatives obtained in periodic calculations with those from oligomeric estimations. Given that the 6-311++G** basis set is too large to perform vibrational frequency calculations for long oligomeric chains, we have used the 6-31G basis set for this comparison. The oligomeric results are calculated by the difference scheme which is less prone to edge effects

$$\frac{\partial \mathbf{d}}{\partial \mathbf{R}_i} = \left(\frac{\partial \mathbf{d}}{\partial \mathbf{R}_i} \right)^{(N)} - \left(\frac{\partial \mathbf{d}}{\partial \mathbf{R}_i} \right)^{(N-1)}, \quad (36)$$

where

$$\left(\frac{\partial \mathbf{d}}{\partial \mathbf{R}_i} \right)^{(N)} = \sum_{m=1}^N \frac{\partial \mathbf{d}}{\partial \mathbf{R}_i^{(m)}}, \quad (37)$$

here, the indices i and m enumerate atoms within a molecule and molecules within an oligomer, respectively. Numerical periodic results are obtained by calculating finite differences between unit cell dipole moments in different geometrical configurations. As expected, oligomeric calculations need more molecules to converge in the periodic direction than in the others. The same trend can be seen in analytic periodic calculations with respect to the number of \mathbf{k} points. The numerical PBC calculation is less sensitive to the number of \mathbf{k} points, however, they have a fixed error due to the finite difference scheme of differentiation. This suggests that the periodic dipole moment converges faster than its derivatives with the number of \mathbf{k} points.

As a matter of practical interest we illustrate the dependence of the five normal mode frequencies and their IR intensities on the number of \mathbf{k} points involved in the discretization of the Brillouin zone with HF and DFT (see Table III). As a representative DFT method we used the non-empirical generalized gradient approximation (GGA) functional of Perdew-Burke-Ernzerhof³¹ (PBE). These model calculations suggest that 100 - 1000 \mathbf{k} points are enough to obtain IR intensities converged within 1%. A large difference in sensitivity of vibrational frequencies and IR intensities to N_k should not be considered as a serious issue, since the overhead from enlarging N_k is negligible in our vibrational frequency evaluation algorithm.⁴ We suppose that the large difference in magnitudes of HF and PBE IR intensities

TABLE II: Comparison of dipole derivatives with respect to Cartesian coordinates of the oxygen atom (in a.u.) for periodic and oligomeric calculations of the water chain with HF (see Fig. 1).

Method	$\partial d_z/\partial O_z$	$\partial d_z/\partial O_y$	$\partial d_y/\partial O_z$	$\partial d_y/\partial O_y$
Basis 6-31G				
Oligomeric $n/n - 1$				
32/31	-1.02563	-0.08673	-0.12885	-0.51942
52/51	-1.02580	-0.08675	-0.12885	-0.51942
82/81	-1.02585	-0.08676	-0.12885	-0.51942
102/101	-1.02587	-0.08676	-0.12885	-0.51942
Numerical (PBC)				
$N_k = 1\ 000$	-1.02611	-0.08664	-0.12872	-0.51931
$N_k = 10\ 000$	-1.02611	-0.08664	-0.12872	-0.51931
Analytic (PBC)				
$N_k = 1\ 000$	-1.02581	-0.08670	-0.12885	-0.51942
$N_k = 10\ 000$	-1.02590	-0.08676	-0.12885	-0.51942
Basis 6-311++G**				
Numerical (PBC)				
$N_k = 1\ 000$	-0.83322	-0.09828	-0.08772	-0.54018
$N_k = 10\ 000$	-0.83322	-0.09826	-0.08772	-0.54018
Analytic (PBC)				
$N_k = 1\ 000$	-0.79599	-0.10754	-0.08496	-0.53669
$N_k = 10\ 000$	-0.79627	-0.10774	-0.08496	-0.53669

is related to the tendency of pure DFT functionals to yield a more metallic description than the HF method.

B. Poly(paraphenylenevinylene)

In order to illustrate the prediction capabilities of our approach, we chose the experimentally and theoretically well-studied one-dimensional system of poly(paraphenylenevinylene) (PPV, Fig. 2).^{10,32,33,34} Such an interest is motivated by conductivity and luminescent nonlinear properties which make this system a promising candidate as a material for light-emitting

TABLE III: Convergence of vibrational frequencies (cm^{-1}) and IR intensities (km/mol) with the number of \mathbf{k} points (N_k) for the five normal modes of the water chain in HF and PBE (see Fig. 1). Band gaps are denoted by E_g .

N_k	1		2		3		4		5	
	Freq.	Int.	Freq.	Int.	Freq.	Int.	Freq.	Int.	Freq.	Int.
HF/6-311++G**, $E_g = 14.4$ eV										
30	399.0	92.0	585.8	271.7	1785.3	146.2	4069.0	208.5	4211.9	79.2
50	399.0	92.8	585.8	271.7	1785.3	146.6	4069.0	210.8	4211.9	79.7
100	399.0	93.3	585.8	271.7	1785.3	147.0	4069.0	212.6	4211.9	80.1
1000	399.0	93.7	585.8	271.7	1785.3	147.4	4069.0	214.1	4211.9	80.4
10 000	399.0	93.8	585.8	271.7	1785.3	147.5	4069.0	214.2	4211.9	80.5
PBE/6-311++G**, $E_g = 5.3$ eV										
30	503.6	75.8	544.6	192.7	1630.9	157.9	3489.0	426.6	3789.1	34.8
50	503.6	76.7	544.6	192.7	1630.9	157.2	3489.0	446.5	3789.1	35.0
100	503.6	77.3	544.6	192.7	1630.9	156.9	3489.0	461.4	3789.1	35.0
1000	503.6	77.8	544.6	192.7	1630.9	156.6	3489.0	474.6	3789.1	35.0
10 000	503.6	77.9	544.6	192.7	1630.9	156.6	3489.0	475.9	3789.1	35.0

diodes.³² We would like to point out that previous theoretical work from our group on PPV was done with some limitations which are overcome in the current study. In Ref. 10, the IR intensities took into account only the changes in the non-periodic part of the dipole moment (d_1). This caused an underestimation of IR intensities for those vibrations that modify the longitudinal dipole moment of PPV.

As mentioned in the Introduction, IR intensities usually receive less attention and their values are presented only graphically in arbitrary units.^{33,34} Therefore, in Table IV we compare IR-active calculated vibrational frequencies with their experimental counterparts. Note that in the case of IR intensities only a qualitative comparison with experimental data can be done (see Fig. 3). In our calculations we used the following functionals: the local spin density approximation³⁵ (LSDA), the meta-GGA of Tao-Perdew-Staroverov-Scuseria³⁶ (TPSS), TPSS hybrid³⁶ (TPSSh), and long-range corrected hybrid PBE³⁷ (LC- ω PBE). Our choice was motivated by a previous study of the performance of the TPSS functional in molecules and solids.^{4,38} We also included the LC- ω PBE functional because we expect some overesti-

mation of IR intensities by regular functionals due to the well-known problem with electric field response properties in extended systems.^{39,40} According to Table IV and Fig. 3, all functionals perform quite adequately, although they generally underestimate lower frequencies and overestimate higher ones. Mean absolute errors with respect to experimentally observable frequencies indicate that the pure DFT methods (LSDA and TPSS) describe vibrational frequencies better than the hybrid functionals (TPSSh and LC- ω PBE). Calculated values of IR intensities qualitatively follow the right trends in most of the cases. It is remarkable that even though LC- ω PBE does not perform very well for vibrational frequencies, it predicts IR intensities which are in a better agreement with experiment than are those from the regular functionals. This complies with the idea that IR intensities with regular functionals suffer mostly from the wrong asymptotic behavior of the exchange potential. It is possible that the correct $1/r$ asymptotic behavior of the LC- ω PBE exchange potential³⁷ is responsible for the improvements of IR intensities in elongated systems.

IV. FINAL REMARKS

We have presented a simple route to evaluating IR intensities in solids within the HF and DFT frameworks with localized basis sets. As in the molecular case, to evaluate IR intensities one needs to differentiate the dipole moment with respect to nuclear coordinate displacements. However, the periodic dipole moment is not a straightforward generalization of its molecular counterpart but rather can be seen as a geometric quantum phase. Thus, we have used the discretized Berry phase expression for the dipole moment per unit cell developed in the modern theory of polarization^{5,6} and elaborated for localized basis sets by Kudin and coworkers.²⁵ We have differentiated the discretized dipole moment expression with respect to in-phase nuclei displacements and have demonstrated validity of our technique on the model one-dimensional chain of water molecules. The evaluation of IR intensities introduces only a negligible overhead in the characterization of vibrational frequencies, since CPU timings for dipole derivatives [Eqs. (29), (32), and (35)], in all studied cases constitute less than 4 % of total CPU times. The PPV study with different functionals reveals that

TABLE IV: PPV IR active vibrational frequencies (cm^{-1}) and their intensities (km/mol) calculated with various methods and the 6-31G** basis set. In all calculations $N_k = 1000$ was used.

Mode ^b	LSDA		TPSS		TPSSh		LC- ω PBE		Expt. ^a
	Freq.	Int.	Freq.	Int.	Freq.	Int.	Freq.	Int.	Freq.
A_u	224	0.2	225	0.2	230	0.2	241	0.2	
B_u	422	26.5	421	23.6	426	19.8	431	7.1	429
A_u	552	11.3	555	9.7	564	10.4	584	12.2	555(s) ^c
B_u	795	30.8	788	31.0	797	27.2	809	12.4	785
A_u	818	27.9	830	31.4	843	32.9	877	32.1	837(s)
A_u	911	0.4	941	0.2	959	0.2	1009	1.0	
A_u	948	33.0	981	29.9	997	32.4	1023	37.5	965(s)
B_u	1000	4×10^{-2}	1011	3×10^{-2}	1025	2×10^{-2}	1050	3.2	1013
B_u	1098	8.5	1122	6.3	1137	5.9	1159	7.0	1108
B_u	1200	14.0	1236	2.0	1247	1.7	1240	1.1	1211
B_u	1302	17.3	1300	9.5	1312	9.9	1314	14.3	1271
B_u	1401	63.5	1389	40.2	1401	34.4	1386	15.5	1339
B_u	1467	1.5	1454	7.8	1470	8.1	1497	8.1	1423(s)
B_u	1538	109.6	1539	81.0	1561	79.3	1608	61.8	1518(s)
B_u	3061	135.4	3121	114.3	3156	104.3	3220	62.7	
B_u	3090	60.9	3136	84.9	3171	77.5	3230	38.3	
B_u	3109	20.2	3162	49.7	3197	45.1	3256	21.1	
MAE ^d	21		17		27		43		

^aReferences 33 and 34.

^bThe normal modes are classified according to the crystallographic point group C_{2h} .

^c“(s)” stands for strong bands.

^dMean absolute error with respect to experimentally observed frequencies.

although the calculated vibrational frequency adequately reproduce those from experiment, the corresponding IR intensities do not always follow qualitatively correct trends. Application of the LC- ω PBE functional corrects IR intensities presumably due to the right $1/r$ asymptotic behavior of the LC- ω PBE exchange potential but worsens frequencies. We hope that our scheme and the results reported here will stimulate further functional development in the future.

Acknowledgments

A.F.I. would like to thank K. N. Kudin, T. M. Henderson, and O. Hod for valuable suggestions. This work was supported by the Department of Energy under Grant No. DE-FG02-04ER15523 and by the Welch Foundation.

-
- ¹ S. Baroni, S. de Gironcoli, A. D. Corso, and P. Giannozzi, *Rev. Mod. Phys.* **73**, 515 (2001).
 - ² See for example, <http://www.pwscf.org> and <http://www.abinit.org>.
 - ³ S. Hirata and S. Iwata, *J. Mol. Struct. (Theochem)* **451**, 121 (1998).
 - ⁴ A. F. Izmaylov and G. E. Scuseria, *J. Chem. Phys.* **127**, 144106 (2007).
 - ⁵ R. D. King-Smith and D. Vanderbilt, *Phys. Rev. B* **47**, 1651 (1993).
 - ⁶ R. Resta, *Rev. Mod. Phys.* **66**, 899 (1994).
 - ⁷ S. A. Prosandeev, U. Waghmare, I. Levin, and J. Maslar, *Phys. Rev. B* **71**, 214307 (2005).
 - ⁸ J. Sun, X.-F. Zhou, J. Chen, Y.-X. Fan, H.-T. Wang, X. Guo, J. He, and Y. Tian, *Phys. Rev. B* **74**, 193101 (2006).
 - ⁹ P. Hermet, M. Goffinet, J. Kreisel, and P. Ghosez, *Phys. Rev. B* **75**, 220102(R) (2007).
 - ¹⁰ K. N. Kudin and G. E. Scuseria, *Phys. Rev. B* **61**, 16440 (2000).
 - ¹¹ E. B. Wilson, J. C. Decius, and P. C. Cross, *Molecular Vibrations* (McGraw-Hill Inc., New York, 1955).
 - ¹² J. C. Decius and R. M. Hexter, *Molecular Vibrations in Crystals* (McGraw-Hill Inc., New York, 1977).
 - ¹³ R. Resta, *Phys. Rev. Lett.* **80**, 1800 (1998).
 - ¹⁴ J. Zak, *Phys. Rev. Lett.* **85**, 1138 (2000).
 - ¹⁵ M. V. Berry, *Proc. R. Soc. A* **392**, 45 (1984).
 - ¹⁶ R. Resta, *J. Phys.: Condens. Matter* **12**, R107 (2000).
 - ¹⁷ D. Bishop, F. L. Gu, and B. Kirtman, *J. Chem. Phys.* **114**, 7633 (2001).
 - ¹⁸ B. Kirtman, F. L. Gu, and D. M. Bishop, *J. Chem. Phys.* **113**, 1294 (2000).
 - ¹⁹ M. Springborg and B. Kirtman, *J. Chem. Phys.* **126**, 104107 (2007).
 - ²⁰ N. Sai, K. M. Rabe, and D. Vanderbilt, *Phys. Rev. B* **66**, 104108 (2002).
 - ²¹ R. W. Nunes and X. Gonze, *Phys. Rev. B* **63**, 155107 (2001).
 - ²² S. Baroni and R. Resta, *Phys. Rev. B* **33**, 7017 (1986).
 - ²³ M. S. Hybertsen and S. G. Louie, *Phys. Rev. B* **35**, 5585 (1987).
 - ²⁴ D. Jacquemin, J.-M. André, and B. Champagne, *J. Chem. Phys.* **118**, 3956 (2003).
 - ²⁵ K. N. Kudin, R. Car, and R. Resta, *J. Chem. Phys.* **126**, 234101 (2007).

- ²⁶ A. F. Izmaylov, E. N. Brothers, and G. E. Scuseria, *J. Chem. Phys.* **125**, 224105 (2006).
- ²⁷ P. M. W. Gill, B. G. Johnson, and J. A. Pople, *Int. J. Quantum Chem.* **40**, 745 (1991).
- ²⁸ Gaussian Development Version, Revision E.02, M. J. Frisch, G. W. Trucks, H. B. Schlegel, G. E. Scuseria, *et al.*, Gaussian, Inc., Wallingford CT, 2004.
- ²⁹ SCF and geometry optimization criteria were set to “tight”, which requests root-mean-squared values of 1×10^{-8} and 1×10^{-5} for density matrix change and atomic forces, and DFT quadrature used “ultrafine” grids, a pruned (99,590) grid.
- ³⁰ H. Guo, S. Sirois, E. I. Proynov, and D. R. Salahub, *Theoretical Treatment of Hydrogen Bonding* (Wiley, Chichester, 1997).
- ³¹ J. P. Perdew, K. Burke, and M. Ernzerhof, *Phys. Rev. Lett.* **77**, 3865 (1996).
- ³² J. H. Burroughes, D. D. C. Bradley, A. R. Brown, R. N. Marks, K. Mackay, R. H. Friend, P. L. Burns, and A. B. Holmes, *Nature* **347**, 539 (1990).
- ³³ B. Tian, G. Zerbi, R. Schenk, and K. Mullen, *J. Chem. Phys.* **95**, 3191 (1991).
- ³⁴ D. Rakovic, R. Kostic, L. A. Gribov, and I. E. Davidova, *Phys. Rev. B* **41**, 10744 (1990).
- ³⁵ S. H. Vosko, L. Wilk, and M. Nusair, *Can. J. Phys.* **58**, 1200 (1980).
- ³⁶ J. Tao, J. P. Perdew, V. N. Staroverov, and G. E. Scuseria, *Phys. Rev. Lett.* **91**, 146401 (2003).
- ³⁷ O. A. Vydrov and G. E. Scuseria, *J. Chem. Phys.* **125**, 234109 (2006).
- ³⁸ V. N. Staroverov, G. E. Scuseria, J. Tao, and J. P. Perdew, *J. Chem. Phys.* **119**, 12129 (2003).
- ³⁹ B. Champagne, E. A. Perpète, S. J. A. van Gisbergen, E.-J. Baerends, J. G. Snijders, C. Soubra-Ghaoui, K. A. Robins, and B. Kirtman, *J. Chem. Phys.* **109**, 10489 (1998).
- ⁴⁰ D. Jacquemin, E. A. Perpète, G. Scalmani, M. J. Frisch, R. Kobayashi, and C. Adamo, *J. Chem. Phys.* **126**, 144105 (2007).

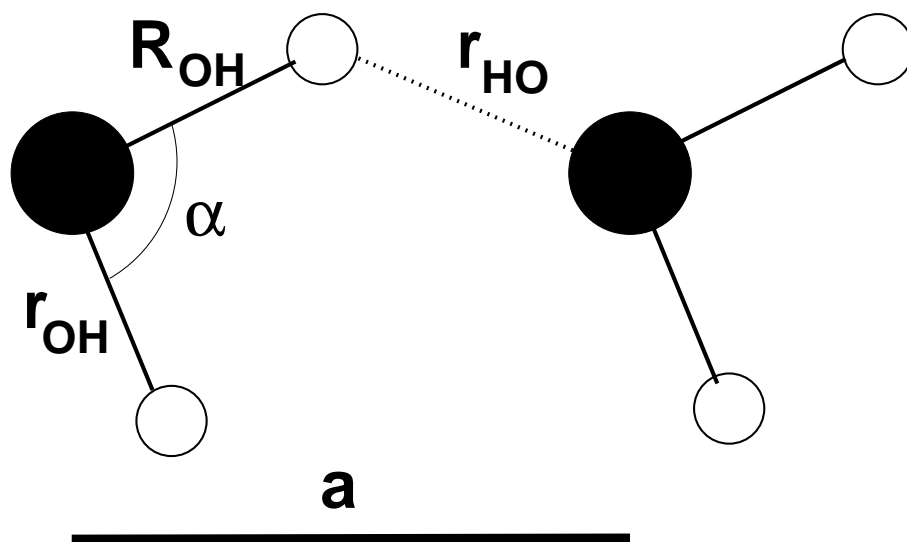


FIG. 1: Schematic structure of the one-dimensional water chain. Optimized parameter values are listed in Table I.

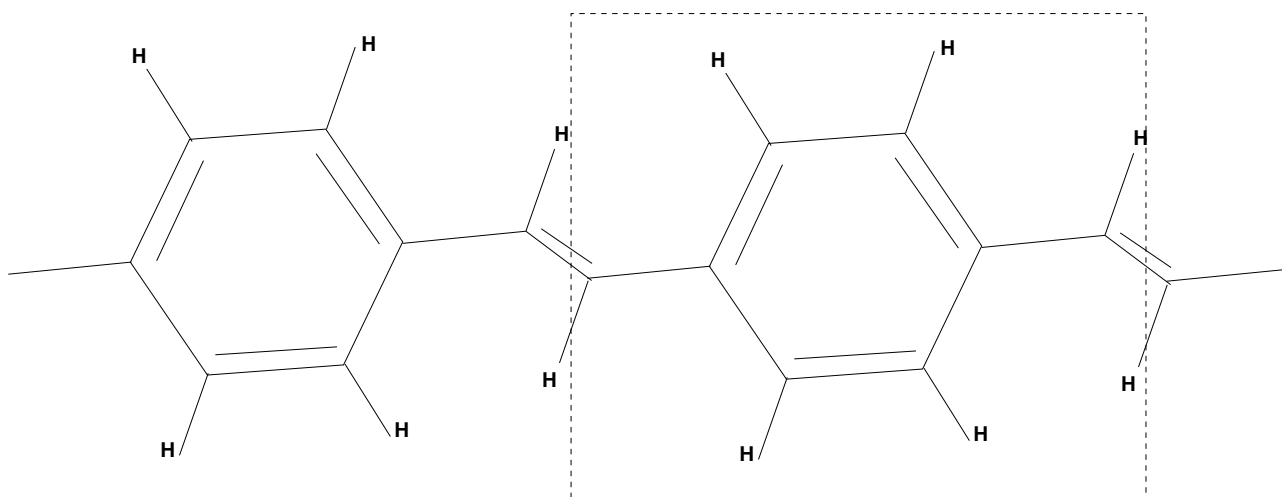


FIG. 2: Poly(paraphenylenevinylene) (PPV).

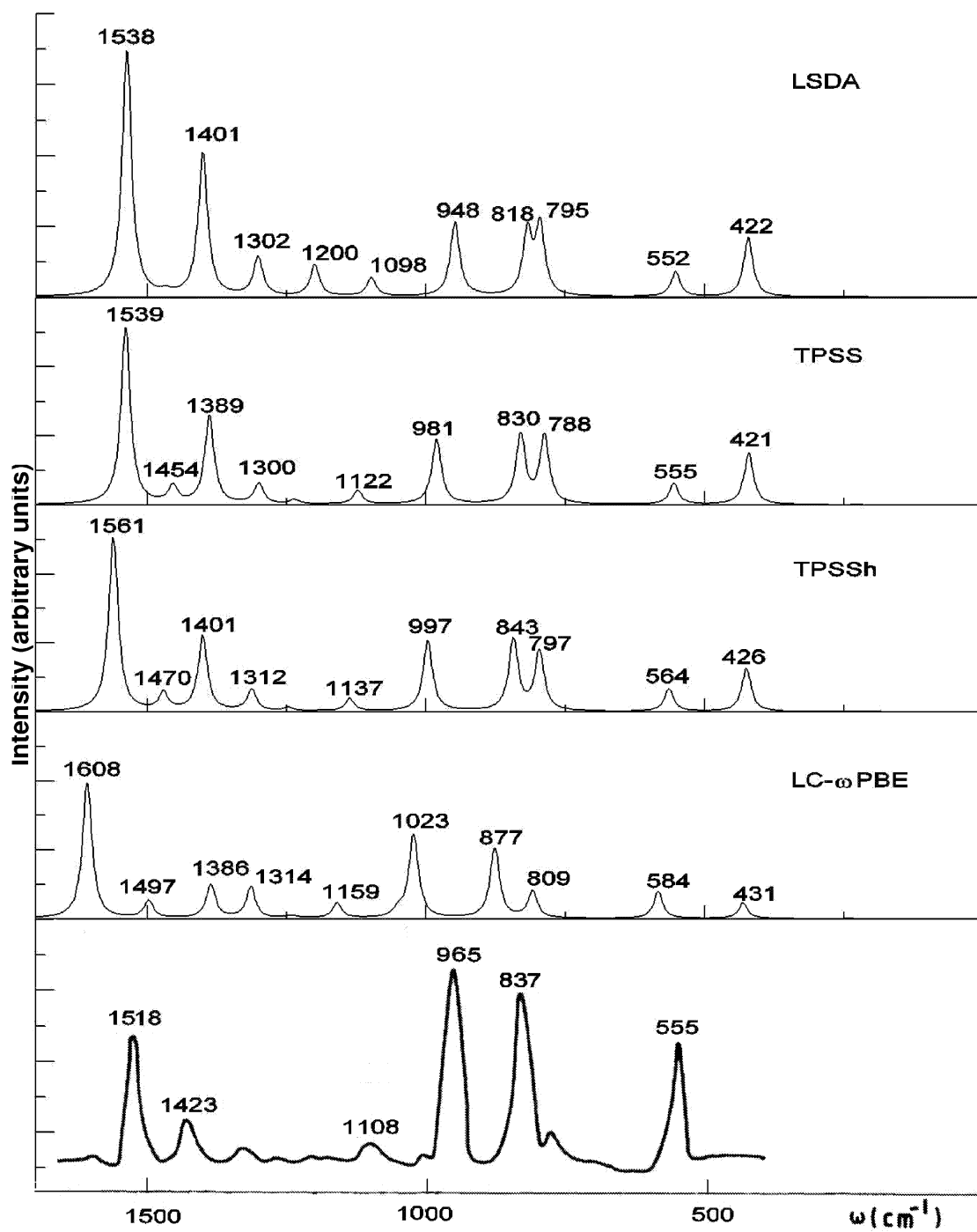


FIG. 3: IR spectra of PPV. The experimental spectrum (bottom graph) is based on data given in Ref. 34. The calculated spectra were obtained by using a Lorentzian broadening with a 10 cm^{-1} width.